

# A novel method for analysis of transient morphological changes in quasiperiodic physiological signals and their neurogenic correlates

Tomasz Gradowski<sup>a</sup>, Damian Wałag<sup>a,b</sup>, Tomir Domański<sup>a,c,d</sup>, Teodor Buchner<sup>a</sup>

<sup>a</sup>*Faculty of Physics, Warsaw University of Technology, Koszykowa 75, Warsaw, 00-662, Poland*

<sup>b</sup>*Center For Digital Medicine, National Institute of Cardiology, Alpejska 42, Warsaw, 04-628, Poland*

<sup>c</sup>*International Centre for Translational Eye Research, Skierniewicka 10A, Warsaw, 01-230, Poland*

<sup>d</sup>*Institute of Physical Chemistry, Polish Academy of Sciences, Kasprzaka 44/52, Warsaw, 01-224, Poland*

---

## Abstract

Frequently, transient changes in physiological signals, such as ECG morphology, precede or follow a rate change. Current methods for visualizing morphology allow only the tracking of preselected changes, severely limiting analytical capabilities. We introduce a novel method for visualizing quasiperiodic signals, enabling the transformation of time series containing repetitive patterns into intuitive visual representations. By using segmentation algorithms and color encoding, we generate two-dimensional "carpet plots" that facilitate simultaneous assessment of heart rhythm and signal features, including the morphology of QRS complexes and T waves, as well as transient changes in intervals and amplitudes. Additionally, the method supports the assessment of concomitant changes in morphology and rate.

Typically, existing visualization methods, such as the standard 12-lead ECG projection, focus either on rhythm variability or on morphological analysis of a few consecutive beats. In contrast, our method integrates both aspects into a single, coherent graphical representation, greatly enhancing the detection of subtle disturbances and a fascinating dynamic interplay between

---

*Email address:* tomasz.gradowski@pw.edu.pl (Tomasz Gradowski)

the rhythm and the morphology of the signal.

We illustrate the effectiveness of this approach using Holter recordings from healthy individuals and patients with arrhythmias, as well as stress test sessions. The results highlight the potential of our visualization technique to support diagnosis and long-term ECG signal analysis. The method may be applied to a broad class of repeatable quasiperiodic patterns - we demonstrate a few examples.

*Keywords:* ECG, quasiperiodic signals, signal processing, signal visualization

---

## 1. Introduction

In signals from many areas of science and technology, quasi-repeating patterns appear, with subsequent forms differing slightly. We may represent this phenomenon as the result of two interacting processes. The first of them determines the time instants of pattern appearances. Formally speaking, this is a point process, also used in physiology [1], a type of stochastic process that defines intervals on the time axis; we refer to it as a rhythmic process. The second process defines the specific pattern and its morphology; we refer to it as the morphological process. Many rhythmic processes can be represented this way: the electrocardiogram, the course of blood pressure, plethysmography, or intracranial pressure and other cardiogenic rhythms in human and animal organisms, the activity of a neuron or their group, patterns in active centers in lasers, forest fires, and other phenomena occurring in active media, often described by spatiotemporal reaction-diffusion equations.

In case of the ECG, the rhythmic process is the well-known Heart Rate Variability (HRV) [2], which is predominantly governed by the autonomous nervous system (ANS) and to much lesser extent by the internal dynamics of the cardiac effector<sup>1</sup>. The rhythmic process is initiated by the sinus node, the heart's natural pacemaker. It undergoes a constant neural and hormonal control [3] which modulates its chronotropic action [4]. This point process is fully described by the sequence of time intervals between successive events in a single realization. For peripheral blood pressure, the interval follows the cardiac cycle and is also affected by pulse transit time [5].

---

<sup>1</sup>Cardiac conductance time affects the PR interval, and hence contributes to the RR interval dynamics - this effect is most often of minor importance.

A morphological process is a description of a single evolution. In the case of the ECG, it represents the electrical activity of the heart muscle. It is a complex spatiotemporal biological and physico-chemical process based on ionic displacements, and executed by the cardiac conductance system and cardiac muscle tissue in response to stimulation. It may be observed via potential imaging [6], surface electrocardiogram (ECG) or magnetocardiogram (MCG) [7] or invasively [8]. In the realm of electronics, there exists a class of monostable multivibrators, which, when triggered, generate a specific pattern, such as an exponential drop to zero. Thus, any dynamics containing quasiperiodic patterns is controlled by two coupled processes: one with continuous time and one with discrete time.

### *1.1. Clinical importance of joint rate-morphology analysis.*

It is interesting to analyze the clinical context using the cardiac morphology and the rate analysis as an example. It is often necessary to understand the coupling between the rhythmic and morphological processes, that is, how momentary changes in timing or frequency translate into morphological alterations.

In the case of the ECG, an example of a transient behavior is the ST elevation or depression [9]. Such an analysis is typically concentrated on a single feature, such as the amplitude of the maximum ST departure from the baseline (elevation or depression). The experienced clinicians know, however, that this is the bottom line of morphology analysis. The ST elevation is essential, but many concomitant changes may accompany this departure: e.g., the wandering of the J point [10], widening of the S wave [11], or even the amplitude of the R wave [12], which also have clinical significance. Typically, a trend of a single feature is tracked [13]. The ability to monitor many trends across different features is technically limited by the visualization method. Correlation with heart rate changes is typically visualized as a 2-D scatterplot.

The changes in morphology may be alternating from beat to beat. ST segment alterations often accompany the ST depression or ST elevation [14]. T wave alternans, which affects every second beat (period doubling) and originates from underlying changes in the action potential duration (APD) [15]. Alternans is a rare event of period doubling with profound consequences for the electrical stability of heart function [16, 17, 18, 19, 20, 21].

In many cases, it is sufficient to look at the signal; however, there also exist certain general-purpose techniques, both in the time and frequency

domains, that are also applied to the ECG morphology assessment, including but not limited to Principal Component Analysis (PCA) [22], Singular Value Decomposition (SVD) [23], Wavelet Transform [24], Poincare Mapping [25], and Fast Fourier Transform (FFT) [26].

Anyway, the changes in morphology may have either simple or more complex beat-by-beat dynamics. If we look at the sole dynamics of the heart rate, it is really rich. Numerous analytical techniques of linear and nonlinear dynamics have been developed to characterize the dynamics of the rhythmic process [2, 27]. These approaches, however, are restricted to rhythm analysis alone, focusing on interval variability while disregarding the signal’s morphological features. There are rare exceptions to this rule in the nonlinear realm [28, 29].

There exists a particularly challenging example of a strong relationship between rhythm and morphology, namely the QT-RR dynamics, which can be studied using a RR-QT diagram [30]. Such a diagram does not allow us to observe changes over time and we lose the possibility to observe whether the trajectory groups around a moving point attractor or rather jumps between distant points. If we look at the cellular-level counterpart of the QT-RR dynamics, the APD/RR or APD/DI analysis reveals important information about the stability of the electrical activity [31]. It is essential to assess the interplay between the rate and the morphology.

## 2. Method

To address the complexities arising from the interaction between rhythmic and morphological processes, we developed a novel method of signal analysis and visualization. This approach enables detailed tracking of how the features of quasi-repeating patterns evolve, capturing both gradual and abrupt morphological changes. By aligning individual pattern realizations based on their rhythmic triggers, the method facilitates the comparison of successive cycles, allowing researchers and clinicians to observe intra- and inter-cycle variability with high temporal resolution. Additionally, it reveals dependencies among parameters, such as amplitude, duration, and waveform shape, within and across cycles. Crucially, the method supports the quantitative assessment of how variations in the frequency or timing of pattern appearances (i.e., rhythmic process fluctuations) influence the morphology of the signal, thereby revealing underlying coupling mechanisms.

We demonstrate the effectiveness of this method using electrocardiogram (ECG) signals, which exhibit clear quasiperiodic structure governed by the cardiac rhythm and rich morphological variability across heartbeats. By applying the proposed analysis framework, individual QRS complexes are extracted and aligned based on R peak timing, enabling precise visualization of morphological dynamics over time. This alignment reveals subtle changes in waveform features such as QRS duration, ST segment elevation, and T wave morphology, features that may indicate physiological adaptations or early signs of pathology. Furthermore, by correlating instantaneous heart rate (derived from R-R intervals) with changes in the shape and amplitude of ECG components, we can quantify the coupling between rhythm variability and morphological responses. This application highlights the method’s potential to enhance diagnostic resolution and monitoring in clinical settings, particularly for arrhythmia detection, stress testing, and autonomic function assessment. It is invaluable for identifying transient changes caused by a chemical imbalance that appear when, at a fast pacing rate of the rhythmic process, the morphological process does not have sufficient time to maintain homeostasis. Note that the coupling is bidirectional: sometimes morphological changes precede rhythm changes; typically, they follow.

It must be stressed that, for the sake of generality, we do not propose any specific diagnostic marker for an electrophysiological symptom of a particular medical condition. We instead demonstrate the approach’s generality, confident that its dissemination will yield much more interesting findings in specific applications.

A limited version of the method has previously been applied to ECG analysis: either in the AF diagnosis context (ECHOView [32]) or in the general ECG context, limited to two consecutive beats (Electrocardiomatrix [33]). We will analyze all the differences between the methods in the Discussion section.

The proposed method is based on a visualization technique that transforms quasiperiodic signals into a graphical representation. The main stages of the procedure are summarized in Fig.1.

To construct the visualization of a signal, the following procedure is applied:

1. Selection of a characteristic feature: The first step is to identify a characteristic feature of the quasiperiodic pattern, typically one that shows high correlation across different realizations.
2. Segmentation of the signal: The signal is segmented into temporal win-

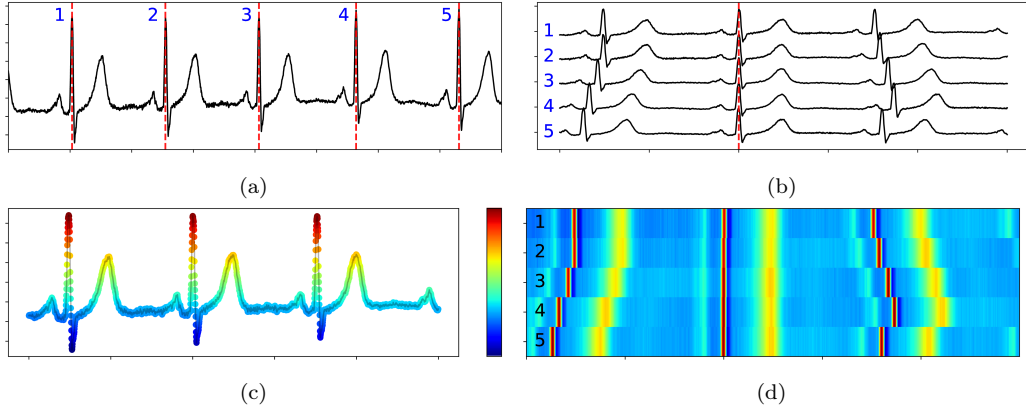


Figure 1: Schematic of the carpet-plot generation procedure. (a) Original ECG signal with marked R peaks; (b) segmented cycles aligned by the central R peak; (c) amplitude-to-color mapping applied within each segment; (d) final "carpet plot" formed by stacking segments in chronological order.

dows based on the identified characteristic points. Each segment is centered around a specific occurrence of the pattern – referred to as the central pattern – and includes either the preceding or following pattern, or both. These segments have a fixed duration, ensuring that the central pattern appears at the same relative position within each segment. This consistency is critical for enabling meaningful comparisons between cycles.

3. Amplitude-to-color mapping: Within each segment, the amplitude value of every sample is mapped to a corresponding color using a predefined transfer function. This mapping can be either linear or nonlinear, depending on the desired sensitivity and contrast. The result is a color representation of the waveform, where subtle amplitude differences become visually distinguishable.

4. Construction of the visualization ("carpet plot"): Finally, all individual segments are stacked vertically in chronological order, aligned by the position of the central pattern, forming a two-dimensional image we refer to as a "carpet plot". In this image, each horizontal line corresponds to a single cycle segment, and the colors along it encode the amplitude values of that segment. The vertical axis represents the progression of cycles over time, while the horizontal axis corresponds to the relative time within each segment.

The above method may be applied to ECG signals, using the R peak as

the characteristic feature for identifying and aligning quasiperiodic patterns. For each detected R peak, a segment of the ECG signal is extracted, spanning a window from e.g. 1 second before to 1.5 seconds after the peak – capturing the full morphological context of the cardiac cycle. This results in segments of uniform duration (2.5 seconds in this case), with the R peak consistently positioned within each segment. Each sample within a segment is then mapped to a color (in this paper, we use the `jet` colormap from the Matplotlib library [34]), which encodes amplitude values across a spectrum from blue (lowest) to red (highest). The segments are subsequently arranged vertically in time order to form a carpet plot, where each horizontal line corresponds to a single heartbeat and its surrounding context. The resulting visualization enables rapid inspection of how ECG morphology evolves, with carpet plot durations ranging from a few minutes (e.g., 3 minutes) to long-term recordings (e.g., 24 hours).

The following Python code snippet illustrates the implementation of the carpet plot generation process:

```
def make_carpet(ecg, rpeaks, preR, postR):
    return [color_scale[ecg[r-preR:r+postR]] for r in rpeaks]
```

In this code, `ecg` is the input ECG signal, `rpeaks` is a list of indices corresponding to detected R peaks, and `preR` and `postR` define the number of samples before and after each R peak to include in the segments. The function constructs a two-dimensional array in which each row corresponds to a segment centered on an R peak, enabling subsequent visualization. Note, that the boundary checks in above code snippet are omitted for clarity.

While the selected parameters used in this study provide a practical and effective configuration, they are not fixed and can be adjusted to suit specific analytical goals or clinical requirements. In particular, the pre-R interval can be shortened if needed. However, it is crucial to ensure the P wave is fully captured, as it contains diagnostically significant information about atrial activity. The post-R interval may be extended in exceptional cases, such as in patients with severe bradycardia, where cardiac cycles are prolonged. Additionally, while the `jet` colormap offers high visual contrast, grayscale colormaps may be preferable in specific contexts, especially when figures are to be printed without color, as they maintain readability and preserve essential morphological distinctions.

Another important point to address is the baseline problem. It is known that one of the typical sources of noise in ECG recordings is baseline wan-

dering, which may result from variable relative impedance between the electrodes that constitute the ECG lead. If this noise is not cancelled during signal processing, it may be removed, e.g., by setting the mean value of the PQ segment to zero, as typically done in Holter recordings. Then, naturally, this value becomes a setpoint for the whole color scale. Other options are also possible, e.g., setting the mean value of each segment to zero.

To further enhance the readability of carpet plots, especially when working with long-term ECG recordings such as Holter monitor data or stress test signals, which are often affected by artifacts, it is helpful to apply amplitude clipping during color mapping. This involves limiting the range of signal values mapped to colors, effectively suppressing extreme outliers that can distort the visual representation. A practical approach is to clip amplitude values based on percentiles; for example, map only values within the 1st-99th percentile range of the entire signal. Values below the lower bound and above the upper bound are then assigned the colors corresponding to those respective limits. This technique preserves the visibility of typical morphological features while minimizing the influence of transient noise or artifacts, making subtle patterns easier to discern across hundreds or thousands of cycles. It is beneficial when comparing ECG morphology over extended periods, where maintaining consistent contrast is crucial for practical interpretation.

Another important consideration arises when carpet plots are used not only for visual inspection but also as inputs to automated analysis pipelines, such as machine learning or pattern recognition algorithms. In such cases, it is essential to maintain a constant number of rows across all carpet plots. This means that a fixed number of segments must be selected. When working with datasets that include signals recorded at different sampling rates, it is equally important to standardize the number of columns in the carpet plots – that is, the number of samples per segment. Since each segment corresponds to a fixed temporal window (e.g., 2.5 seconds), variations in sampling frequency will result in different segment lengths unless corrected. To ensure consistency, all signals must be resampled to a common target sampling rate before visualization. This preprocessing step ensures that each segment contains the same number of data points and, therefore, that each carpet plot has a uniform width (number of columns). Ensuring uniform input dimensions is a fundamental requirement for most machine learning models, particularly convolutional neural networks (CNNs), which expect input tensors of consistent shape.

In order to demonstrate the merits of the method, we have applied it to se-

lected recordings from THEW database E-HOL-03-0480-013 [35], MIT-BIH Atrial Fibrillation Database [36], INCART database [37], EPHNOGRAM database [38] and CHARIS database [39]. The presented carpet plots were generated using custom-built software that allows analysis of signals in various formats [40].

### 3. Results

To assess the effectiveness of the proposed visualization method, we applied it to ECG recordings from multiple publicly available databases. The chosen datasets varied in both recording length and sampling rate, demonstrating the method’s robustness across heterogeneous acquisition settings. Notably, the examples included patients with diverse cardiac conditions, such as inherited arrhythmia syndromes, atrial fibrillation, and exercise-induced changes, highlighting the versatility of carpet plots in capturing both rhythm irregularities and morphological dynamics. The results are presented in Fig. 2.

To demonstrate the impact of color mapping as a research tool, we present an example of a II-degree AV block with Wenckebach periodicity in the standard and adjusted color scales 4. The rate of change of the PQ interval can be assessed by direct measurement of the angle of the oblique line. As conduction through the AV node becomes increasingly impaired, given a specific mean HR (also visible in the carpet view), this rate of change is a convenient measure of the imbalance, enabling quantification of this pathology. Hence, color-scale adjustments allow focusing on specific dynamical features.

Since the method is novel, special attention must be paid to the interpretation of carpet plots. The vertical axis represents successive cardiac cycles, aligned with both absolute time (HH:MM:SS) and RR interval indices. This dual labeling supports interpretation across short (minutes) and long (hours or even 24-hour) recordings. For example, Fig. 2 shows signals ranging in length from about 7 minutes (Fig. 2a) to about 25 minutes (Fig. 2d), while Fig. 6 shows a recording fragment lasting about 2 hours. This method also allows for quickly assessing signals lasting 24 hours without losing any information from the original signal. Because RR intervals vary, the vertical scale in real time is, in fact, nonlinear. Each row is anchored at the R position, and the difference between them is the RR interval, which is highly variable. The horizontal axis represents relative time within each cycle and is displayed on a linear scale. In our study, we used a 2.5-second window (1 second before

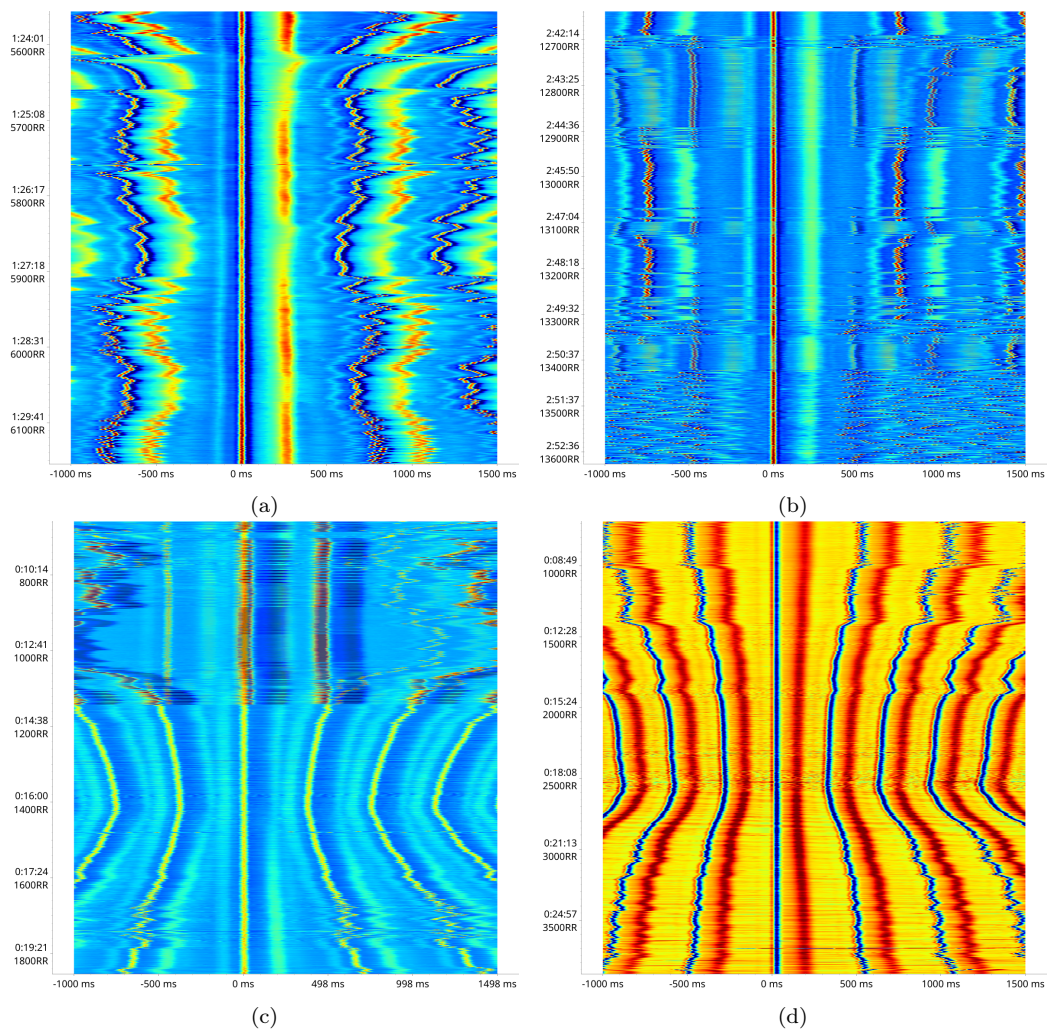


Figure 2: Examples of carpet plots for different ECG signals. (a) male, 19 years old, diagnosed with LQT1 (patient #174 from THEW database E-HOL-03-0480-013 [35]); (b) patient #08405 from MIT-BIH Atrial Fibrillation Database [36]; (c) record I51 (lead II) from INCART database [37]; (d) record #36 of stress-test session from EPHNOGRAM database [38]

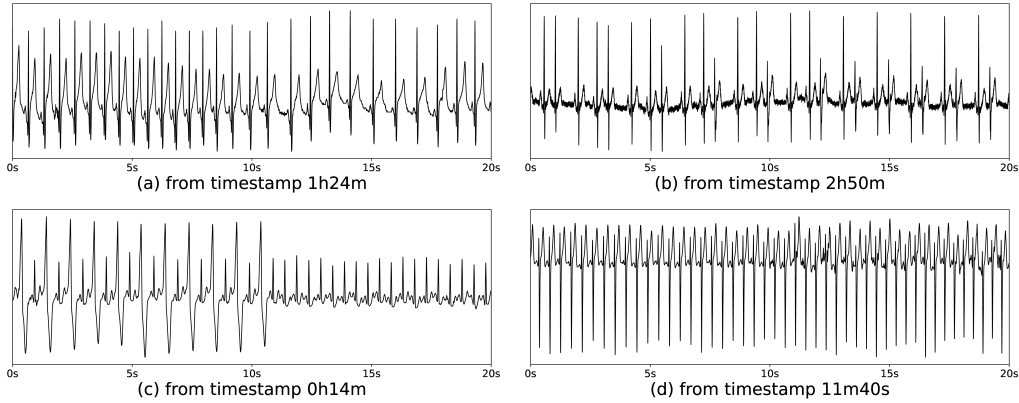


Figure 3: Representative 20-second raw ECG signal segments corresponding to the carpet plots in Fig.2.

and 1.5 seconds after the R wave), adjusted slightly depending on sampling rate.

Heart rate patterns (and the corresponding RR intervals with their dynamics) are easily inferred by examining the position of the next R wave relative to the central R wave. This allows rapid estimation of tachograms directly from the carpet. When rotated 90 degrees counterclockwise, the carpets resemble conventional heart rate variability plots (tachograms), facilitating interpretation. Stress test recordings (e.g., Fig. 2, bottom-right) illustrate this clearly, with intervals of baseline rest, exercise at stepwise-increasing load, and recovery easily distinguishable, clearly showing the test protocol. Arrhythmic events, including atrial fibrillation (Fig. 2b) or premature ventricular contractions (PVCs) in bigeminy and trigeminy patterns (Fig. 2c), are also readily identifiable.

To facilitate interpretation, Fig.3 shows the corresponding 20-second raw ECG fragments for each dataset presented in Fig.2. These short signal excerpts highlight the characteristic morphological patterns – such as QRS shape, T wave amplitude, and baseline variations – that, when visualized over longer durations, give rise to the textures and color patterns observed in the carpet plots. By comparing Figures 2 and 3, one can directly relate the features of the original waveform to their manifestation in the two-dimensional representation.

Morphological changes are visible as vertical structures, most prominently the QRS complexes and subsequent T waves. Color coding enables the de-

tection of subtle variations in amplitude, duration, or waveform shape. For instance, in the case of long QT syndrome (Fig. 2a), carpets reveal abrupt changes in T wave morphology and QT interval length, correlated with heart rate variations. The same patient also exhibits changes in the PQ interval, manifested as variations in the width of the blue band between the P wave and the QRS.

All these changes are also visible in the ECG. However, the carpet plot is, in our opinion, much better suited for the reality of an automatic ML-based event detection pipeline: note that all the findings presented in Fig. 2 were selected from large datasets by visual inspection, which was fast and effective, concentrated on departures from a typical pattern, i.e., the anomalies.

Carpet plots also reveal phase transitions in rhythm and morphology. Fig. 2d shows a recording from a stress test, where the subsequent phases of the test are clearly visible: rest phase, stress (of varying intensity), and recovery. Within each of these phases, distinct differences are visible in the rhythm (slower and more strongly correlated with breathing at rest, faster but more stable during stress) and morphology (e.g., shortening of the QT interval during stress). Phase transitions can also be abrupt (discontinuous). For example, the recording in Fig. 2b shows a patient who suddenly experiences an episode of atrial fibrillation. Fig. 2c shows a recording in which PVCs suddenly disappear when an episode of supraventricular tachycardia occurs.

Other, more subtle phenomena observed in the carpets include ST segment depression and elevation. These are manifested by a change in color or intensity on either side of the T wave (c.f. Fig. 2a). This allows for precise observation of episodes of ischemia and the changes related not only to the elevation or depression of the ST segment, but also transient changes of the QRS complex morphology and the level of the J point, which typically pose a challenge for ST algorithms performing automated analysis.

Note that typically in the II degree block, we consider the variable PQ segment within a constant RR interval; however, due to altered AV conduction time, both the PQ interval and the RR interval are prolonged, as rising PQ increases the RR. This effect is marked by oblique line segments: solid for the consecutive P wave peaks and dashed for the R peaks during the intermittent block episode. This is a subtle electrophysiological effect, typically not considered, as in standard projection, it is barely visible. Even in a standard color map, it may be easily left unattended. Additionally, the R peak at 0 ms exhibits an island-like structure, originating from strong respiratory modulation of the R amplitude, also visible in the ECG.

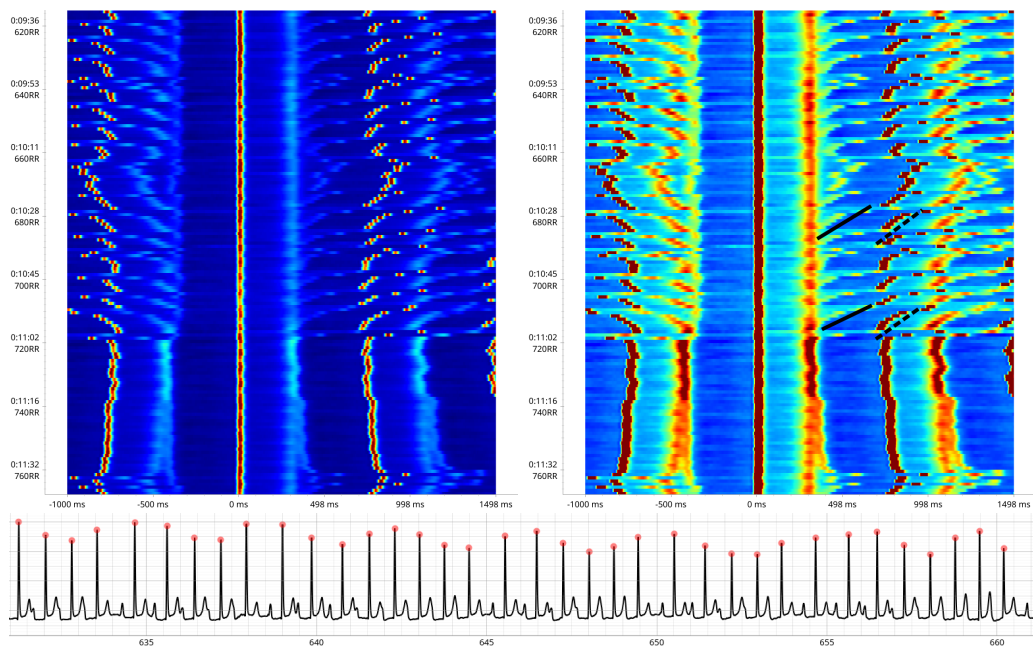


Figure 4: Carpet plots of a patient diagnosed with 2nd degree AV nodal block (record I11 from INCART database). Comparison of two different color mappings: with a top and bottom half-percentile cutoff (left) and manual adjustment to focus on the amplitude range typical to both T wave and P wave (right). Wenckebach periodicity is clearly visible.

## 4. Discussion

A key contribution of the proposed method is its integration of two distinct analytical approaches that, until now, have been mainly treated in isolation, as we further discuss in the cardiological context. The first approach focuses on rhythm characteristics, including HRV and the statistical properties of RR intervals, as well as possible rhythm disturbances, providing insights into autonomic regulation and cardiovascular dynamics. The second approach, in contrast, focuses on morphological features of individual cardiac cycles – such as the shape, amplitude, and duration of QRS complexes, T waves, or ST segments – which are often analyzed to detect structural or electrophysiological abnormalities. In the standard 12-lead projection, the latter approach is applied to a single evolution or to multiple evolutions. In contrast, the former one requires a longer strip of a single selected electrode, typically lead II. Concerning the transient changes of certain features, they are typically analysed as time series: one series per feature. Moreover, their choices are limited, as there is typically no good reason to consider, e.g., the elevation or depression of the J point. In consequence, this type of analysis is not included in the equipment used in clinics, even for 12-lead Holter recordings. In a scientific context, we can study as many features as we want. If the morphology is rich, as in the presented ECG examples, the number of time series required to faithfully reflect the complex changes grows rapidly, and it becomes more cumbersome to find correlations between the observed features. By enabling simultaneous, temporally aligned analysis of both rhythm and morphology, our method bridges these two domains. The structure of the carpet plot, which aligns morphological data to rhythmically defined anchor points (i.e., R peaks), allows for the direct visualization and quantification of correlations between cycle-to-cycle timing variability and morphological changes. This opens up new possibilities for studying the coupling mechanisms between both processes, the rhythmic and the morphological, and for reasoning about causality, for example, whether variations in heart rate induce changes in waveform shape, or vice versa. Such joint analysis provides a richer, more holistic understanding of physiological dynamics, particularly in complex conditions where both timing and shape are affected.

Another important strength of our method is its suitability for both qualitative and quantitative analysis. From a qualitative perspective, the carpet plot provides a highly intuitive and condensed representation of even very long-term physiological signals, making it significantly more accessible for

human interpretation than traditional raw signal plots. This is particularly valuable in scenarios involving extended recordings, such as 24-hour Holter ECGs or multi-phase stress tests, where visual analysis of the raw waveform is impractical. A single glance at a carpet plot can reveal high-level patterns, for instance, transitions between rest and activity, changes in heart rate variability, or periods of stable versus irregular morphology, such as, e.g., episodes of paroxysmal atrial fibrillation. Sleep stages, physical exertion, or transient episodes of autonomic imbalance become immediately apparent, offering clinicians rapid insight without exhaustive signal scrolling or the use of any single-purpose algorithm. The abovementioned features make the carpet plot a convenient tool for exploratory analysis when it is not known in advance what kinds of changes will be elicited by changes in heart rate and its morphological footprint.

Simultaneously, the same carpet plot structure naturally lends itself to quantitative analysis using computational methods. Since the plots are two-dimensional, image-like representations with uniform structure, they are especially well-suited for processing by modern machine learning techniques, including convolutional neural networks (CNNs), vision transformers (ViT), and other pattern recognition models. The popular algorithms for automatic feature detection will easily identify more changes and their correlates than even a highly trained operator. This approach has been recently utilized in the AF detection context by Krasteva *et al.* [32].

To illustrate this potential, we applied a ResNet18 model [41] pretrained on ImageNet set [42] to one of the carpet plots and visualized the resulting feature maps (Fig. 5). Even without training a dedicated classifier, the network was able to extract a variety of distinct patterns, emphasizing that convolutional filters naturally respond to characteristic frequency-domain structures present in the data, as explained by the convolution theorem. Our aim here is not to propose a specific classification model, but rather to demonstrate the feasibility of such integration. The clear differentiation of features across convolutional layers underscores the promise of combining carpet plot visualizations with convolutional networks or other AI-based methods to support automated analysis and anomaly detection.

Moreover, this representation aligns well with explainable AI (XAI) frameworks, enabling visual attribution of model decisions to specific regions of the carpet plot – thus supporting transparent, interpretable classification or anomaly detection. In this way, our method serves as a unified platform that supports both expert-driven interpretation and automated, data-driven

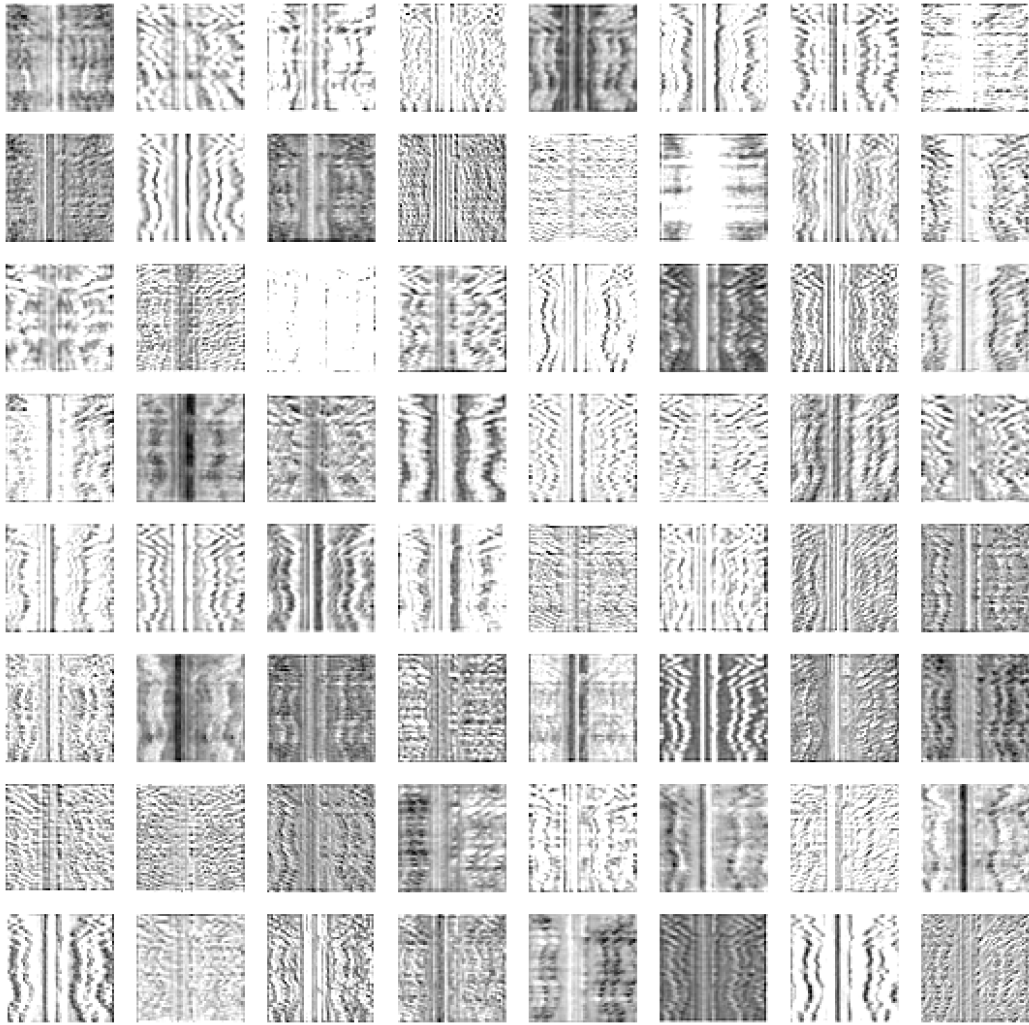


Figure 5: Feature maps extracted from carpet plot of LQTS patient (Fig. 2a) using ResNet18 model (first 3 convolutional layers).

discovery.

An additional advantage of the proposed method is its ability to operate across multimodal signals, provided they are recorded simultaneously and properly synchronized. In such cases, the characteristic feature used for segmentation (e.g., R peaks) and the signal from which the segments are extracted and visualized can originate from different sources. For example, R peaks detected in a single ECG lead, such as Lead I, can serve as the temporal anchors for segmenting signals from other ECG channels, such as the precordial leads (V1-V6), allowing for comparative visualization of spatial cardiac activity. This allows us to easily identify the epochs of transient episodes of decreased conductance, which mainly affect the dispersion of QRS duration. A separate paper on this subject is in preparation.

Finally, the same R peaks can be used to segment non-electrical physiological signals recorded in parallel, such as arterial blood pressure (ABP) or intracranial pressure (ICP). This approach enables the construction of carpet plots that reflect the dynamic coupling between cardiac rhythm and other physiological systems, providing a powerful tool for analyzing cardiovascular-cerebrovascular interactions, autonomic regulation, and more. By decoupling the reference feature from the target signal, the method supports flexible, synchronized exploration of complex biological processes (Fig. 6). The idea to apply the method to other biological signals, the method of alignment on PQ segment, and the nonlinear map for color coding of signal levels are the original contributions of the current paper, which distinguishes it from both [33] and [32], that we became aware of at the time of writing.

## 5. Conclusion

In this work, we introduce a novel method for visualizing quasiperiodic signals by transforming them into carpet plots, which compactly represent both rhythmic and morphological variability across successive cycles, using a selected color mapping. Applied to ECG recordings, the approach enables simultaneous inspection of heart rate dynamics and waveform morphology, thereby overcoming the limitations of traditional 12-lead ECG projections that typically address these aspects in isolation.

Beyond their immediate diagnostic value, carpet plots also provide an adequate representation of input for computational analysis. Their image-like structure is well-suited for integration with modern machine learning techniques. This dual applicability – to human-driven exploration and AI-based

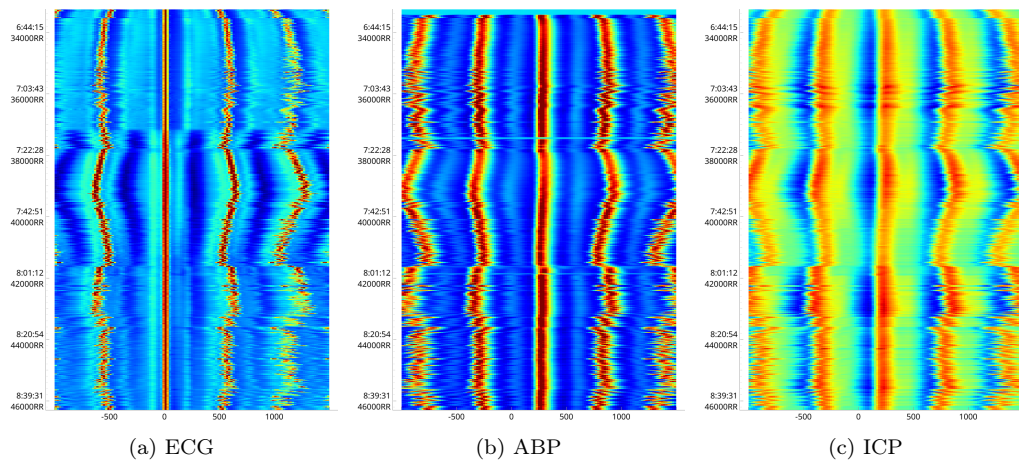


Figure 6: Synchronized carpet plots of ECG, ABP, and ICP signals from the CHARIS database [39] (record #2).

pattern discovery – positions the method as a promising tool for advancing automated, explainable, and scalable analysis of ECG and other quasiperiodic signals.

Looking forward, we demonstrate how the technique may be extended to multimodal physiological recordings, offering a unified framework for studying coupling across different organ systems. By bridging qualitative and quantitative domains, carpet plots have the potential to enhance both routine diagnostics and research into complex dynamical processes in physiology.

## 6. Acknowledgements

Rafał Baranowski is acknowledged for his remarks, particularly for the PQ-based normalization idea. Mateusz Ozimek and Monika Petelczyc are thanked for the data. Natalia Dziura is thanked for testing.

## References

- [1] R. G. Turcott, S. B. Lowen, E. Li, D. H. Johnson, C. Tsuchitani, M. C. Teich, A nonstationary poisson point process describes the sequence of action potentials over long time scales in lateral-superior-olive auditory neurons, *Biological Cybernetics* 70 (3) (1994) 209–217. doi:10.1007/bf00197601.

- [2] Task Force of the European Society of Cardiology and the North American Society of Pacing and Electrophysiology, Heart rate variability: Standards of measurement, physiological interpretation, and clinical use, *Circulation* 93 (5) (1996) 1043–1065. doi:10.1161/01.cir.93.5.1043.
- [3] M. Boyett, The sinoatrial node, a heterogeneous pacemaker structure, *Cardiovascular Research* 47 (2000) 658–687. doi:10.1016/S0008-6363(00)00135-8.
- [4] P. H. Brubaker, D. W. Kitzman, Chronotropic Incompetence, *Circulation* 123 (9) (2011) 1010–1020. doi:10.1161/CIRCULATIONAHA.110.940577.
- [5] S. Hoshida, A. Yoshihisa, F. Tsuchida, H. Mizuno, H. Teragawa, T. Kasai, H. Koito, S.-I. Ando, Y. Watanabe, Y. Takeishi, K. Kario, Pulse transit time-estimated blood pressure: a comparison of beat-to-beat and intermittent measurement, *Hypertens. Res.* 45 (6) (2022) 1001–1007. doi:10.1038/s41440-022-00899-z.
- [6] I. R. Efimov, V. P. Nikolski, G. Salama, Optical imaging of the heart, *Circulation Research* 95 (1) (2004) 21–33. doi:10.1161/01.RES.0000130529.18016.35.
- [7] K. Pęczalski, J. Sobiech, T. Buchner, T. Kornack, E. Foley, D. Janczak, M. Jakubowska, D. Newby, N. Ford, M. Zajdel, Synchronous recording of magnetocardiographic and electrocardiographic signals, *Scientific Reports* 14 (12 2024). doi:10.1038/s41598-024-54126-5.
- [8] P. Kuklik, L. Szumowski, J. J. Żebrowski, P. Sanders, Integration of the data from electroanatomical mapping system and CT imaging modality, *The International Journal of Cardiovascular Imaging* 25 (4) (2009) 425–432. doi:10.1007/s10554-008-9394-1.
- [9] G. S. Wagner, P. MacFarlane, H. Wellens, M. Josephson, A. Gorgels, D. M. Mirvis, O. Pahlm, B. Surawicz, P. Kligfield, R. Childers, L. S. Gettes, AHA/ACCF/HRS recommendations for the standardization and interpretation of the electrocardiogram: Part VI: Acute ischemia/infarction: A scientific statement from the American Heart Association Electrocardiography and Arrhythmias Committee, Council on Clinical Cardiology; The American College of Cardiology Foundation;

And the Heart Rhythm Society, *Circulation* 119 (10) (2009) 262–270. doi:10.1161/CIRCULATIONAHA.108.191098.

- [10] M. J. Junttila, S. J. Sager, J. T. Tikkanen, O. Anttonen, H. V. Huikuri, R. J. Myerburg, Clinical significance of variants of J-points and J-waves: early repolarization patterns and risk, *European Heart Journal* 33 (21) (2012) 2639–2643. doi:10.1093/eurheartj/ehs110.
- [11] A. T. de Andrade, R. Barbosa-Barros, K. Nikus, R. D. Raimundo, L. C. de Abreu, L. Sacilotto, F. C. Darrioux, F. G. Yanowitz, P. Brugada, A. R. Pérez-Riera, Transient ascending ST-segment depression and widening of the S wave in 3-channel Holter monitoring—A sign of dromotropic disturbance in the right ventricular outflow tract in the Brugada syndrome: A report of five cases, *Annals of Noninvasive Electrocardiology* 27 (2) (2022) 1–6. doi:10.1111/anec.12917.
- [12] M. Andrzejewska, M. Ozimek, K. Rams, T. Buchner, Asymmetry of RR intervals and ECG amplitudes in LQTS patients, in: 2022 12th Conference of the European Study Group on Cardiovascular Oscillations (ESGCO), IEEE, 2022, pp. 1–2. doi:10.1109/ESGCO55423.2022.9931345.
- [13] P. Bjerregaard, A. El-Shafei, S. L. Kotar, A. J. Labovitz, ST segment analysis by Holter Monitoring: Methodological considerations, *Annals of Noninvasive Electrocardiology* 8 (3) (2003) 200–207. doi:10.1046/j.1542-474X.2003.08306.x.
- [14] K. M. Kessler, E. J. Bauerlein, A. Schob, E. de Marchena, R. J. Myerburg, ST-alternans alternans, *Am. J. Cardiol.* 70 (13) (1992) 1224–1225. doi:10.1016/0002-9149(92)90065-7.
- [15] L. Glass, P. Hunter, A. McCulloch (Eds.), *Theory of Heart*, Springer New York, 1991. doi:10.1007/978-1-4612-3118-9.
- [16] S. M. Narayan, T-wave alternans and the susceptibility to ventricular arrhythmias, *Journal of the American College of Cardiology* 47 (2) (2006) 269–281. doi:10.1016/j.jacc.2005.08.066.
- [17] T. Krogh-Madsen, D. J. Christini, Action potential duration dispersion and alternans in simulated heterogeneous cardiac tissue with a structural barrier, *Biophysical Journal* 92 (4) (2007) 1138–1149. doi:10.1529/biophysj.106.090845.

- [18] J. M. Starobin, C. P. Danford, V. Varadarajan, A. J. Starobin, V. N. Polotski, Critical scale of propagation influences dynamics of waves in a model of excitable medium, *Nonlinear Biomedical Physics* 3 (2009) 1–7. doi:10.1186/1753-4631-3-4.
- [19] M. J. Cutler, D. S. Rosenbaum, Explaining the clinical manifestations of T wave alternans in patients at risk for sudden cardiac death., *Heart rhythm* 6 (3 Suppl) (2009) S22–8. doi:10.1016/j.hrthm.2008.10.007.
- [20] A. L. Aro, T. V. Kenttä, H. V. Huikuri, Microvolt T-wave Alternans: Where Are We Now?, *Arrhythmia & Electrophysiology Review* 5 (1) (2016) 37. doi:10.15420/aer.2015.28.1.
- [21] M. Gabr, S. Mangeshkar, L. Cerna, K. Rahgozar, M. H. Al-Taei, M. Grushko, Abstract 11663: T Wave Alternans: A Clue in Plain Sight, *Circulation* 148 (Suppl\_1) (nov 2023). doi:10.1161/circ.148.supp\_1.11663.
- [22] P. M. Okin, R. B. Devereux, R. R. Fabsitz, E. T. Lee, J. M. Galloway, B. V. Howard, Principal component analysis of the T Wave and prediction of cardiovascular mortality in american indians, *Circulation* 105 (2002) 714–719. doi:10.1161/hc0602.103585.
- [23] M. Andersen, J. Xue, C. Graff, T. Hardahl, E. Toft, J. Kanters, M. Christiansen, H. Jensen, J. Struijk, A robust method for quantification of IKr-related T-wave morphology abnormalities, in: *2007 Computers in Cardiology*, IEEE, 2007, pp. 341–344. doi:10.1109/CIC.2007.4745491.
- [24] M. V. Gualsaquí Miranda, I. P. Vizcaíno Espinosa, M. J. Flores Calero, ECG signal features extraction, in: *2016 IEEE Ecuador Technical Chapters Meeting (ETCM)*, 2016, pp. 1–6. doi:10.1109/ETCM.2016.7750859.
- [25] F. Li, J. Zhao, H. L. Jia, C. Y. Zhang, X. L. Zhu, Poincare mapping: A potential method for detection of T-wave alternans, in: *Procedia Environmental Sciences*, Vol. 8, Elsevier B.V., 2011, pp. 575–581. doi:10.1016/j.proenv.2011.10.089.
- [26] R. Maniewski, P. Lewandowski, M. Nowinska, T. Mroczka, Time-frequency methods for high-resolution ECG analysis, in: *Proceed-*

- ings of 18th Annual International Conference of the IEEE Engineering in Medicine and Biology Society, Vol. 3, 1996, pp. 1266–1267 vol.3. doi:10.1109/IEMBS.1996.652804.
- [27] U. Rajendra Acharya, K. Paul Joseph, N. Kannathal, C. M. Lim, J. S. Suri, Heart rate variability: a review (Nov. 2006). doi:10.1007/s11517-006-0119-0.
- [28] R. Baranowski, J. J. Żebrowski, Assessment of the RR versus QT relation by a new symbolic dynamics method, *Journal of Electrocardiology* 35 (2) (2002) 95–103. doi:10.1054/jelc.2002.32414.
- [29] M. Baumert, M. Javorka, M. Kabir, Joint symbolic dynamics for the assessment of cardiovascular and cardiorespiratory interactions, *Philosophical Transactions of the Royal Society A: Mathematical, Physical and Engineering Sciences* 373 (2034) (2015) 20140097. doi:10.1098/rsta.2014.0097.
- [30] M. Malik, Relation between QT and RR intervals is highly individual among healthy subjects: implications for heart rate correction of the QT interval, *Heart* 87 (2002) 220–228. doi:10.1136/heart.87.3.220.
- [31] H. M. Hastings, F. H. Fenton, S. J. Evans, O. Hotomaroglu, J. Geetha, K. Gittelsohn, J. Nilson, A. Garfinkel, Alternans and the onset of ventricular fibrillation, *Physical Review E* 62 (3) (2000) 4043–4048. doi:10.1103/physreve.62.4043.
- [32] V. Krasteva, T. Stoyanov, S. Naydenov, R. Schmid, I. Jekova, Detection of atrial fibrillation in holter ECG recordings by ECHOView images: A deep transfer learning study, *Diagnostics* 15 (4 2025). doi:10.3390/diagnostics15070865.
- [33] D. Li, F. Tian, S. Rengifo, G. Xu, M. M. Wang, J. Borjigin, Electrocardiomatrix: A new method for beat-by-beat visualization and inspection of cardiac signals, *Journal of Integrative Cardiology* 1 (2015). doi:10.15761/jic.1000133.
- [34] J. D. Hunter, Matplotlib: A 2d graphics environment, *Computing in Science & Engineering* 9 (2007) 90–95. doi:10.1109/MCSE.2007.55.

- [35] J. P. Couderc, The telemetric and holter ECG warehouse initiative (THEW): A data repository for the design, implementation and validation of ECG-related technologies, in: 2010 Annual International Conference of the IEEE Engineering in Medicine and Biology Society, EMBC'10, 2010, pp. 6252–6255. doi:10.1109/IEMBS.2010.5628067.
- [36] G. Moody, R. Mark, A new method for detecting atrial fibrillation using R-R intervals, *Computers in Cardiology* (1983) 227–230.
- [37] A. L. Goldberger, L. A. N. Amaral, L. Glass, J. M. Hausdorff, P. C. Ivanov, R. G. Mark, J. E. Mietus, G. B. Moody, C.-K. Peng, H. E. Stanley, PhysioBank, PhysioToolkit, and PhysioNet, *Circulation* 101 (6 2000). doi:10.1161/01.CIR.101.23.e215.
- [38] A. Kazemnejad, P. Gordany, R. Sameni, Ephnogram: A simultaneous electrocardiogram and phonocardiogram database (2021). doi:10.13026/TJTQ-5911.
- [39] N. Kim, A. Krasner, C. Kosinski, M. Wininger, M. Qadri, Z. Kappus, S. Danish, W. Craelius, Trending autoregulatory indices during treatment for traumatic brain injury, *Journal of Clinical Monitoring and Computing* 30 (2016) 821–831. doi:10.1007/s10877-015-9779-3.
- [40] ECG carpets, <https://github.com/tomgrad/carpets> (2025).
- [41] K. He, X. Zhang, S. Ren, J. Sun, Deep residual learning for image recognition, in: 2016 IEEE Conference on Computer Vision and Pattern Recognition (CVPR), IEEE, 2016, pp. 770–778. doi:10.1109/CVPR.2016.90.
- [42] J. Deng, W. Dong, R. Socher, L.-J. Li, K. Li, L. Fei-Fei, Imagenet: A large-scale hierarchical image database, in: 2009 IEEE Conference on Computer Vision and Pattern Recognition, IEEE, 2009, pp. 248–255. doi:10.1109/CVPR.2009.5206848.